

TABLE OF CONTENTS

	Page
Acknowledgement	iii
Abstract (in English)	v
Abstract (in Thai)	vii
List of Tables	xiii
List of Figures	xv
Abbreviations and symbols	xxi
CHAPTER 1 INTRODUCTION	1
1.1 General introduction to supramolecular interactions	5
1.1.1 Hydrogen bond	5
1.1.2 Halogen bond	7
1.1.3 Aromatic π - π interactions	9
1.1.4 Aliphatic CH/ π interactions	11
1.2 Synthesis and single crystal growth techniques	14
1.2.1 Diffusion method	14
1.2.2 Solvo(hydro)thermal synthesis	15
1.2.3 Microwave-assisted synthesis	16
1.2.4 Ionothermal synthesis	18
1.3 Polycarboxylate and amino acids as ligands	19
1.4 Research objectives	23

1.5 Research plan	24
CHAPTER 2 NEW POLYMORPH OF 1,3,5-TRIAZINE-2,4,6- TRIAMINEHEXAACETIC ACID	30
2.1 Experimental	31
2.1.1 Microwave-assisted crystal growth of TTHA-II	31
2.1.2 Structure determination and refinement	32
2.1.3 Vibrational and electronic spectroscopic study of TTHA-II	33
2.2 Results and discussion	34
2.2.1 Crystal structure and hydrogen bonding network analysis of TTHA-II	34
2.2.2 Spectroscopic study of TTHA-II	40
2.3 Conclusions	41
CHAPTER 3 NEW TRINUCLEAR Ni^{II} COMPLEX CONTAINING INCOMPLETE CUBANE Ni₃O₄ CORE STRUCTURE	44
3.1 Experimental	45
3.1.1 Synthesis and crystal growth	45
3.1.2 Single crystal structure determination	45
3.2 Results and discussion	51
3.3 Conclusions	57
CHAPTER 4 A CHIRAL DECORATED METAL-NICOTINATE FRAMEWORK	61
4.1 Experimental	62

4.1.1 Microwave–assisted hydrothermal crystal growth and initial characterization	62
4.1.2 Structure determination and refinement	63
4.2 Results and discussion	68
4.2.1 Description of crystal structures	68
4.2.2 The FT–IR spectrum and thermal behaviors	73
4.3 Conclusions	75
CHAPTER 5 IONOTHERMAL SYNTHESIS AND CRYSTAL STRUCTURES OF NEW d^{10} BLUE LUMINESCENT METAL–ORGANIC MATERIALS	77
5.1 Experimental	79
5.1.1 Synthesis and characterization	79
5.1.2 Single crystal structure determination	80
5.1.3 Structure and property of the de–intercalated samples	86
5.2 Results and discussion	86
5.2.1 Crystal structures description	86
5.2.2 Thermogravimetric analysis	97
5.2.3 UV–Vis and photoluminescent spectroscopic studies	98
5.2.4 Stability and photoluminescence property of the de–intercalated IV–L and V–L	101
5.3 Conclusions	106
CHAPTER 6 CONCLUSIONS	110

APPENDICES

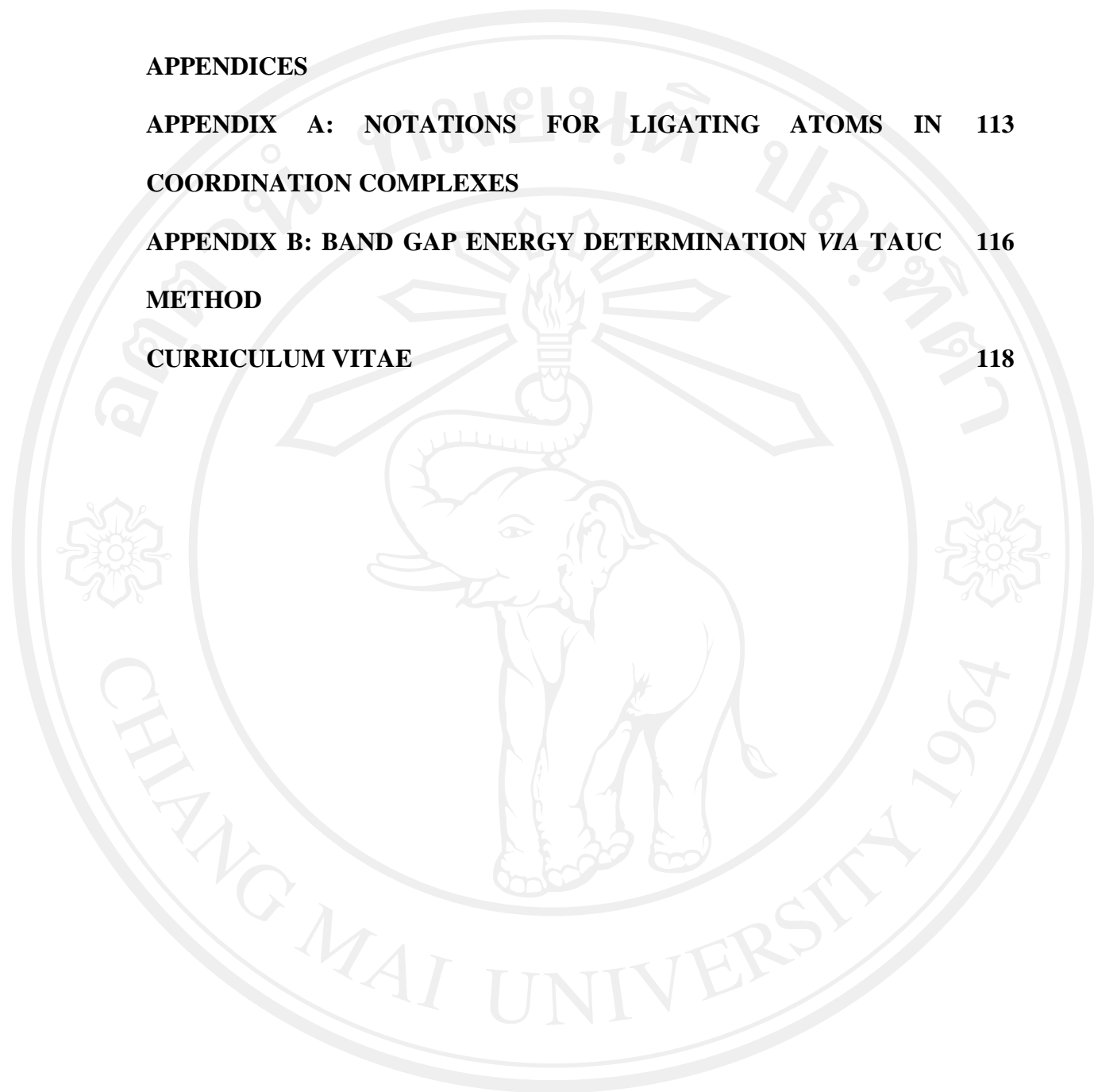
APPENDIX A: NOTATIONS FOR LIGATING ATOMS IN 113

COORDINATION COMPLEXES

APPENDIX B: BAND GAP ENERGY DETERMINATION VIA TAUC 116

METHOD

CURRICULUM VITAE 118



ลิขสิทธิ์มหาวิทยาลัยเชียงใหม่

Copyright© by Chiang Mai University
All rights reserved

LIST OF TABLES

Table		Page
1.1	Classification of hydrogen bonding interactions.	5
1.2	Distance and orientation dependence of the CH/ π interactions.	12
2.1	Crystal and experimental data for TTHA-I and TTHA-II .	33
2.2	Selected geometric parameters for TTHA-II .	34
2.3	Details of the hydrogen bonding interactions in TTHA-II . A hydrogen bond donor and acceptor are denoted as D and A, respectively.	37
3.1	Crystallographic data for structural solution and refinement of I .	46
3.2	Atomic coordinates and equivalent isotropic displacement parameters of non-hydrogen atoms for I .	47
3.3	Selected observed bond distances and angles in the compound I .	50
3.4	Hydrogen bonding geometry for I .	55
4.1	Crystal and experimental data for II and III .	64
4.2	Atomic coordinates and equivalent isotropic displacement parameter for II .	65
4.3	Atomic coordinates and equivalent isotropic displacement parameter for III .	66
4.4	Selected bond distances and angles in II .	67

4.5	Selected bond distances and angles in III .	67
4.6	Details of the hydrogen bonding interactions in II . A hydrogen bond donor and acceptor atoms are denoted as D and A, respectively.	71
5.1	Crystal and experimental data for IV and V .	81
5.2	Atomic coordinates and equivalent isotropic displacement parameter for IV .	82
5.3	Atomic coordinates and equivalent isotropic displacement parameters for V .	83
5.4	Selected geometric parameters for IV .	85
5.5	Selected geometric parameters for V .	85
5.6	Details of the hydrogen bonding interactions in IV . A hydrogen bond donor and acceptor are defined as D and A, respectively.	94
5.7	FT-IR and Raman assignments for IV , V , IV-L and V-L .	96

LIST OF FIGURES

Figure		Page
1.1	Metal–organic materials encompass discrete (0–D) as well as extended structures with periodicity in one (1–D), two (2–D) and three (3–D) dimensions.	2
1.2	Representation of (a) 1–D, (b) 2–D and (c) 3–D MOMs.	3
1.3	Appropriate choices of ligands in providing (a) coordination compounds and (b) coordination networks.	4
1.4	Representation of hydrogen bonding interactions (dotted line) of (a) $[\text{Co}^{\text{II}}(\text{C}_2\text{H}_2\text{N}_2)_3]\text{SO}_4$ [19] and (b) $\text{M}_3(\text{BTC})_2 \cdot 12\text{H}_2\text{O}$.	6
1.5	Diagrams showing the presence of halogen bond (dotted line) in a series of Hg(II) complexes.	8
1.6	Representations of (a) the presence of halogen bonds in the zigzag chain structure of the co–crystals of (1,2–diiodoterfluorobenzene)·(phenazine) and (b) the halogen and hydrogen bonds in the structure of (2–mercapto–1–methylimidazole)·(1,2–diiodoterfluorobenzene).	9
1.7	Principal orientations of aromatic–aromatic or π – π interactions.	10

- 1.8 Representation of (a) π - π and $\text{CH}\cdots\pi$ interactions in 10
 $[\text{Ni}(\text{Phen})_2(\text{H}_2\text{O})_2][\text{Ni}(\text{PtcH})_2]\cdot 11\text{H}_2\text{O}$ and (b) the 2-D framework structure with hydrophilic cavities formed by strong π - π and $\text{CH}\cdots\pi$ interactions.
- 1.9 Formation of two isomeric supramolecular architectures. Each isomer 11
consists of 2-D honeycomb layers based on 4,4',4''-(2,4,6-trimethylbenzene-1,3,5-triyl)tribenzoic acid (H_3TMTA) and $\text{Zn}_2(\text{COO})_3$ SBUs.
- 1.10 Representation of the existence of the aliphatic CH/π interactions in 13
the crystal structure of $\{[\text{Zn}(\text{L})_2\text{Cl}_2]\cdot\text{DMF}\cdot\text{CH}_3\text{OH}\}_n$; L is 1,4-bis(benzimidazol-1-ylmethyl)benzene.
- 1.11 Representation of (a) crystal packing of the acetate compound 13
showing the 3-D network of microchannels (backbone blur) and (b) a cavity with the aliphatic chains pointing toward it.
- 1.12 Representation of (a) liquid diffusion and (b) vapor diffusion methods. 14
- 1.13 Diagram showing the components of general hydrothermal reactor. 16
- 1.14 Dipolar molecules trying to align with an oscillating electric field of 17
microwave component.
- 1.15 Some typical cations and anions commonly used as the component of 18
ILs.
- 1.16 Diagrams showing different coordination modes of carboxylate 20
groups.
- 1.17 A large series of isorecticular IRMOFs. 20

- 1.18 Coordination modes of TTHA in (a) $\{\text{Na}_2[\text{Co}_3(\text{H}_2\text{TTHA})_2(\text{H}_2\text{O})_{12}] \cdot (\text{H}_2\text{O})_2\} \cdot 4\text{H}_2\text{O}$, (b) $\{\text{Na}[\text{Cu}_4(\text{H}_2\text{TTHA})(\text{HTTTHA})(\text{H}_2\text{O})_8](\text{H}_2\text{O})_3\} \cdot 5\text{H}_2\text{O}$, (c) $[\text{Cd}_3(\text{TTHA})(\text{H}_2\text{O})_4]$ and (d) $[\text{Ca}_5(\text{HTTTHA})_2(\text{H}_2\text{O})_8]$. 22
- 2.1 ORTEP drawing of molecular unit in **TTHA-II** showing atom numbering scheme and 70% probably displacement ellipsoids for non-hydrogen atoms. Symmetry code: (i) - $x, y, 1.5 - z$. 35
- 2.2 Hydrogen bonding interactions (dotted lines) in **TTHA-II** illustrated by (a) capped stick model showing intermolecular interactions, (b) 70% thermal ellipsoids showing intramolecular interactions, and (c) capped stick model showing the packing of molecular units. 36
- Symmetry codes: (i) - $x, y, 1.5 - z$; (ii) - $x, 2 - y, 2 - z$; (iii) $x, 2 - y, 0.5 + z$; (iv) $0.5 - x, -0.5 + y, 2.5 - z$; (v) $0.5 - x, 2.5 - y, 2 - z$; (vi) - $0.5 + x, 2.5 - y, -0.5 + z$; (vii) - $0.5 - x, 2.5 - y, 1 - z$.
- 2.3 Crystal packing in **TTHA-II** showing (a) face-to-face π -stacking and (b) molecular columns built up from the stacking of the molecules in c -direction. 39
- 2.4 Simulated X-ray diffraction patterns of (a) **TTHA-I** and (b) **TTHA-II**. 39
- 2.5 FT-IR spectrum collected on the ground crystals of **TTHA-II**. 40
- 2.6 UV-Vis spectrum collected on a suspension of the ground **TTHA-II** crystals in methyl alcohol. 41

- 3.1 The asymmetric unit of **I** showing atom-labeling scheme and with 50% probability displacement ellipsoids. Hydrogen atoms are omitted for clarity. 52
- 3.2 The incomplete cubane core of **I**. Only selected atoms from the ligands are drawn. Atoms are shown as 30% probability ellipsoids. 53
- 3.3 View of (a) intra-cluster and (b) inter-cluster hydrogen bonding interactions (dash lines), showing the donor and acceptor atoms by ball-and-stick model and with 50% probability displacement ellipsoids for the incomplete cubane core. Weak C–H...O hydrogen bonding interactions are omitted. 56
- 4.1 View of extended asymmetric units of (a) **II** and (b) **III** with 50% thermal ellipsoids and atomic labeling for non-hydrogen atoms. The hydrogen bond shows in dotted lines. Symmetry code: (i) $x - 1, y, z - 1$. 68
- 4.2 Illustration of the one-dimensional coordination polymer $[\text{Co}(\text{C}_9\text{H}_{10}\text{NO}_3)(\text{C}_6\text{H}_4\text{NO}_2)(\text{H}_2\text{O})_2]_n$ chain within **II**. Color scheme: Ni, black; O, dark grey; N, light grey; C, grey. 69
- 4.3 Views of (a) ABAB stacking of the $[\text{Co}(\text{C}_9\text{H}_{10}\text{NO}_3)(\text{C}_6\text{H}_4\text{NO}_2)(\text{H}_2\text{O})_2]_n$ chains parallel to the b -axis and (b) checkerboard arrangement of the chains along $[1\ 0\ 1]$ direction. 70
- 4.4 Representation of the hydrogen bonding interactions (dotted lines) in **II**, generated by (a) $-x, y - 1/2, -z$, (b) $-x, y - 1/2, -z + 1$ and (c) $x - 1, y, z$ and $x, y, z + 1$. 72
- 4.5 FT-IR spectra collected on the ground crystals of (a) **II** and (b) **III**. 74

4.6	Thermogravimetric analysis of (a) II and (b) III .	74
5.1	Views of the extended asymmetric units of (a) IV and (b) V , showing the tetrahedral–octahedral–tetrahedral trimers. Thermal ellipsoids are shown with 60% probability, and hydrogen atoms are omitted for clarity. Symmetry codes: (i) $2 - x, -1 - y, -z$; (ii) $2 - x, -y, -z$; (iii) $\frac{1}{2} + x, \frac{1}{2} - y, \frac{1}{2} + z$; (iv) $x, 1 + y, 1 + z$; (v) $x, -1 + y, -1 + z$; (vi) $1 - x, -y, 1 - z$; (vii) $2 - x, 1 - y, 2 - z$.	87
5.2	Views of the extended layered structure of (a) IV and (b) V , showing spatial arrangements of the extraframework cations and C–H...O hydrogen bonding interactions (dotted lines). Symmetry codes: (i) $-\frac{1}{2} + x, \frac{1}{2} - y, \frac{1}{2} + z$; (ii) $\frac{3}{2} - x, \frac{1}{2} + y, \frac{1}{2} - z$.	89
5.3	The (3,6) uninodal net of hxl topology or triangular grid of the isorecticular (a) IV and (b) V .	91
5.4	The ABAB stacking of the two–dimensional in IV , intercalated by the extraframework EMI ⁺ cations.	92
5.5	The ABAB stacking of the two–dimensional in V , intercalated by the extraframework BMI ⁺ cations.	93
5.6	FT–IR spectra of (a) IV and (b) V .	95
5.7	Raman spectra of (a) IV and (b) V .	95
5.8	Thermogravimetric curve collected on the ground crystals of (a) IV and (b) V .	97
5.9	UV–Vis spectra of (a) EMI–Cl, (b) H ₂ BDC and (c) IV .	99
5.10	UV–Vis spectra of (a) BMI–Cl, (b) H ₂ BDC and (c) V .	99

5.11	Plots of $(\alpha hv)^2$ value versus photon energy (hv) for (a) IV and (b) V .	100
5.12	Photoluminescent spectra of (a) H ₂ BDC, (b) IV and (c) V .	101
5.13	PXRD patterns calculated from single crystal data of (a) IV compared with those collected on the bulk samples of (b) IV and (c) the de-intercalated IV-L .	102
5.14	PXRD patterns calculated from single crystal data of (a) V compared with those collected on the bulk samples of (b) V and (c) the de-intercalated V-L .	102
5.15	FT-IR spectra of the de-intercalated (a) IV-L and (b) V-L .	103
5.16	Raman spectra of the de-intercalated (a) IV-L and (b) V-L .	104
5.17	Thermogravimetric curves of the de-intercalated (a) IV-L and (b) V-L , compared with those of the prior de-intercalated (c) IV and (d) V , respectively.	105
5.18	Photoluminescent spectra of (a) H ₂ BDC, the de-intercalated (b) IV-L and (c) V-L , compared with those of the prior de-intercalated (d) IV and (e) V , respectively.	105
A.1	Diagrams showing typical coordination modes of (a) carboxylate groups and (b) 1,4-benzenedicarboxylate with corresponding notations.	113
A.2	Diagrams showing typical coordination modes of <i>L-p</i> -tyrosinate ligands with corresponding notations.	114

ABBREVIATIONS AND SYMBOLS

atm	atmosphere
BMIIm	1-butyl-3-methylimidazolium
<i>ca.</i>	<i>circa</i> (approximately)
calc.	calculation
cm	centimeter
cm ³	cubic centimeter
<i>e.g.</i>	<i>exempli gratia</i> (for example)
<i>et al.</i>	<i>et alibi</i>
<i>etc.</i>	<i>et cetara</i>
eV	electron volt
EMIIm	1-ethyl-3-methylimidazolium
FT-IR	fourier transform infrared spectroscopy
g	gram
H ₂ BDC	1,4-benzenedicarboxylic acid (terephthalic acid)
<i>i.e.</i>	<i>id est</i> (that is)
ILs	ionic liquid solvents
IUPAC	International Union of Pure and Applied Chemistry
K	Kelvin
kHz	kilohertz
K/s	Kelvin per second

mA	milliampere
MHz	megahertz
min	minute
mm	millimeter
MOMs	metal–organic materials
nm	nanometer
n/a	not available
PXRD	powder X–ray diffractometry
T	temperature
TTHA	1,3,5–triazine–2,4,6–triaminehexaacetic acid
Tyr	tyrosine
vs.	<i>versus</i>
UV–Vis	ultraviolet–visible spectroscopy
W	Watt
Å	angstrom
°C	degree Celsius
%	percent
θ	theta
ρ	density
μm	micrometer
1–D	one–dimensional
2–D	two–dimensional
3–D	three–dimensional